Supporting Information

Small molecule condensin inhibitors

Hang Zhao, Zoya M. Petrushenko, John K. Walker, Jerome Baudry, Helen I. Zgurskaya, Valentin V. Rybenkov

Table of content

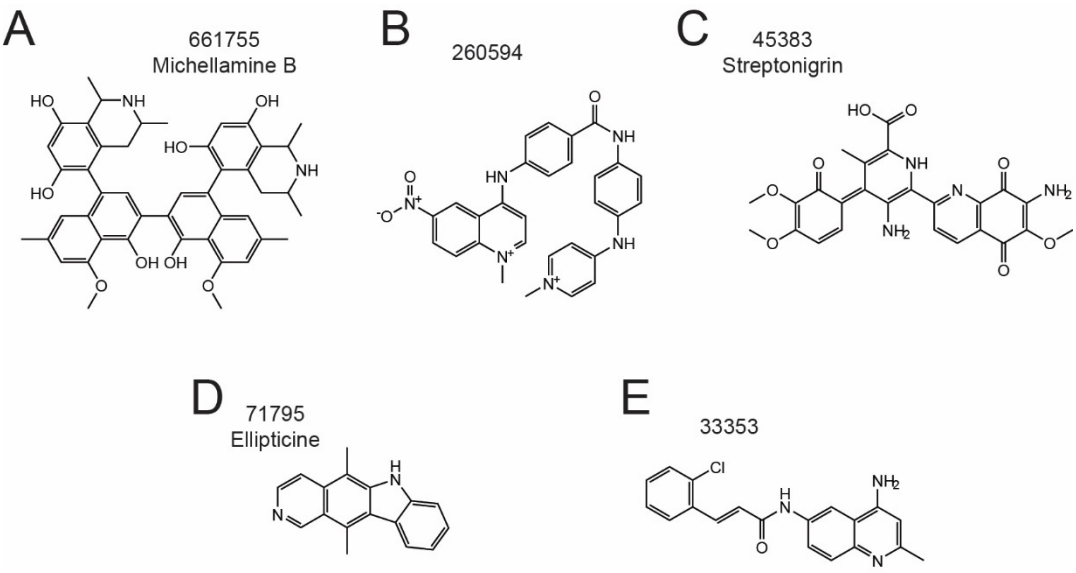

Figure S1. Chemical structure of the hit compounds.

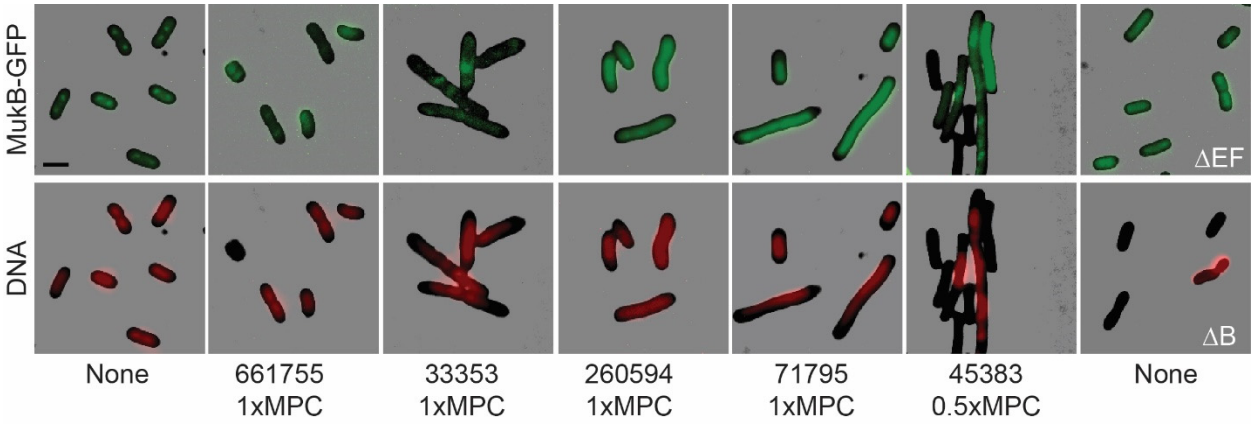

Figure S2. Formation of anucleate and afocal cells upon treatment with the hit compounds. 10,000 exponential *ΔmukEF mukB-gfp* OU152 (ΔEF), *ΔmukB ΔtolC* OU142 (ΔB) or *ΔtolC mukB-gfp* OU151 (otherwise) cells were grown overnight in LB at a permissive temperature (23 °C for OU152 and OU142 cells, 37 °C for OU151 cells), transferred into fresh LB medium, supplemented with the indicated compounds and incubated at 37 °C for 16 hours. Subcellular localization of MukB-GFP was observed using fluorescence microscopy. Anucleate cells were detected as previously described[1] after staining the DNA with DAPI and protein with Sypro Orange. Size bar, 1 μm.

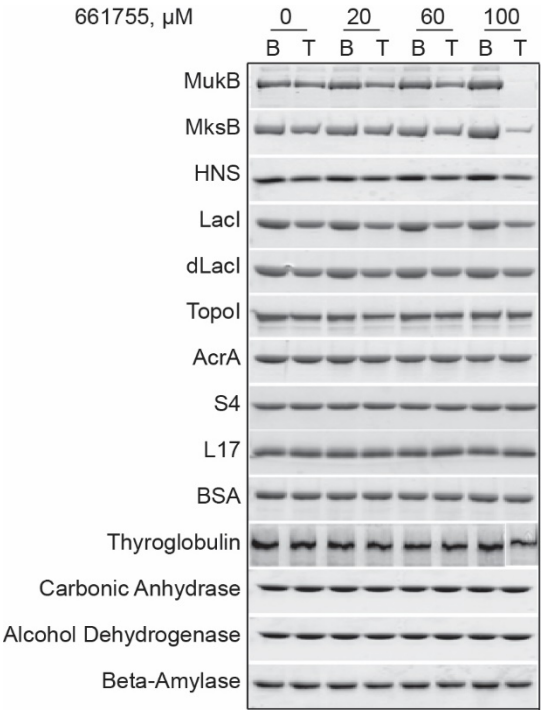

Figure S3. Evaluation of Michellamine-induced protein aggregation. Tested were: *E.coli* MukB, *P. aeruginosa* MksB, *E.coli* HNS, *lac* repressor LacI, the dimeric LacI unable to form tetramers, dLacI, wheat germ topoisomerase I, *E. coli* membrane fusion protein AcrA, ribosomal proteins S4 and L17 from *E. coli*, bovine serum albumin, BSA, and calf thymus thyroglobulin, carbonic anhydrase, alcohol dehydrogenase and β-amylase.

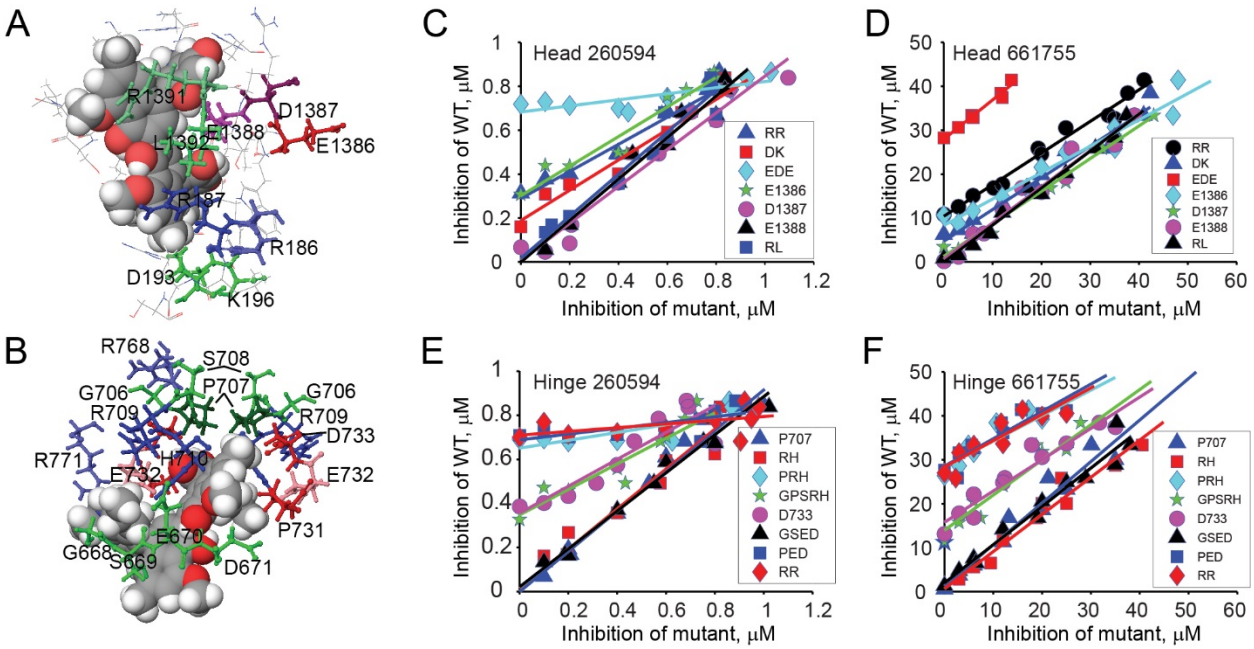

Figure S4. Interaction of Michellamine B and 260594 with the hinge and head domains of MukB. Compounds are shown in spheres, side chains are shown for residues in the binding sites (**A, B**) The interaction environment for Michellamine B in the head (**A**) and hinge (**B**). (**C-F**) Inhibition curves for the hinge and head domain mutants for Michellamine and NSC260594, as indicated.

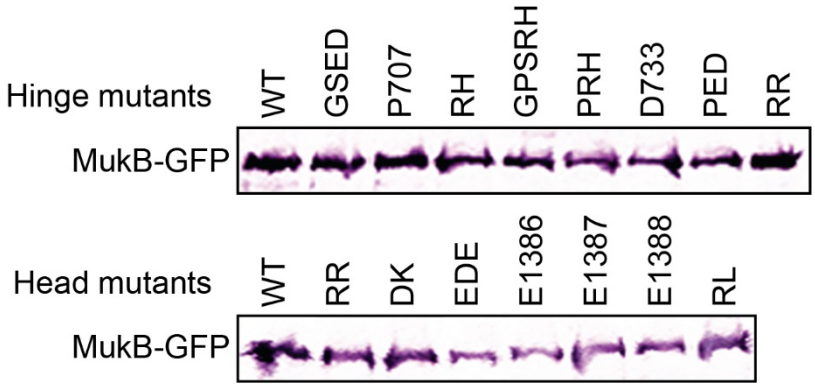

Figure S5. Expression of mutant variants of MukB-GFP from p15sp-B02a plasmid. 0.1 OD of *ΔtolCΔmukB* cells harboring the indicated plasmids were analyzed by immunoblotting using anti-GFP antibody.

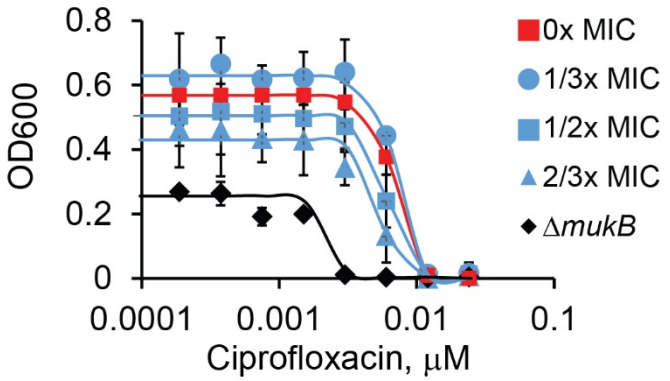

Figure S6. Potentiation of ciprofloxacin by NSC260594 in *ΔtolC E. coli.*

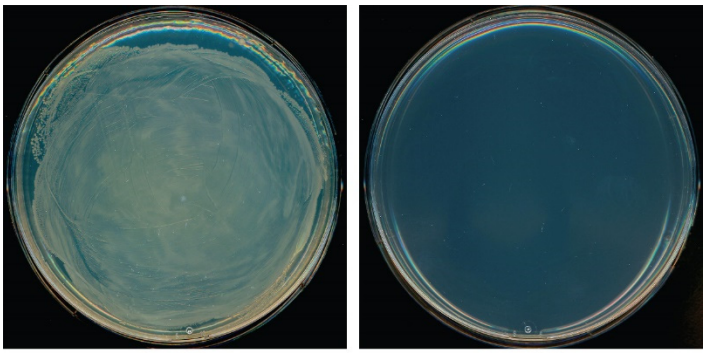

Figure S7. Frequency of spontaneous suppressor mutations. $1.5 \cdot 10^9$ exponential BW25115 *ΔtolC* cells were spread over three LB plates containing the indicated concentration of NSC250594 and incubated for 24 h at 37 ºC.

Table S1. Minimal inhibitory concentrations of the hit compounds in the presence or absence of 1/4x MIC of novobiocin (±SEM; μM).

Compound	*ΔtolC*		*ΔtolCΔmukB*	
	- novo	+ novo	- novo	+ novo
33353	9.2±1	3.3±0.1	4.6±0.6	4.6±0.2
260594	0.87±0.03	0.45±0.01	0.3±0.02	0.33±0.01
661755	33±3	12±0.3	24±0.8	19±4
45383	0.6±0.03	0.34±0.03	0.27±0.01	0.28±0.01
71795	15±2	10±1.5	9.8±0.5	8.4±0.4

Table S2. Minimal inhibitory concentrations of NSC260594 and NSC176319.

Strain	260594, μM (μg/ml)	176319, μM (μg/ml)
E. coli BW25115	32 (16)	20 (13)
E. coli ETBW	2.5 (1.3)	1 (0.6)
P. aeruginosa GKCW122	14 (7)	5 (3)
A. baumannii IL123	3.5 (1.8)	2.5 (1.6)
S. aureus ATCC 25923	28 (14)	10 (6)

Table S3. Strains used in this study.

Strain	Relevant Genotype	Source
E. coli		
MG1655	Wild type *E. coli*	Lab stock
BW25113	Wild type *E. coli*	[2]
ETBW	BW25113 Δ*tolC::*Km^r	[3]
OU142	BW25113 Δ*tolC* Δ*mukB::* Km^r	[4]
OU151	MG1655 Δ*mukB::* Km^r *lacYA::mukB-gfp-spc^r* Δ*tolC::cam*	This study
OU152	MG1655 Δ*mukEF::* Km^r *lacYA::mukB-gfp-spc^r*	This study
Pseudomonas aeruginosa		
PaGKCW111	PAO1 *att*Tn*7*::mini-Tn*7*T-Gm^r-*lacI^q*-pLAC-MCS	[5]
GKCW122	PAO1Δ6 *att*Tn*7*::mini-Tn*7*T- Gm^r-*lacI^q*-pLAC- *fhuA* Δ*C/*Δ*4L*	[5]
Staphylococcus aureus		
SA	*Staphylococcus aureus* subsp. *aureus* Rosenbach ATCC 25923	ATCC
Acinetobacter baumannii		
JWW19	ATCC 17978 *att*Tn*7*::miniTn*7*-Tp^r-*araC*-P$_{araBAD}$-MCS (pTJ1)	[5]
IL123	ATCC 17978 Δ3 *att*Tn*7*::miniTn*7*-Tp^r-*araC*-P$_{araBAD}$-*fhuA*(FhuA$_{\Delta Cork\Delta 4Loop,\ 6His}$) (pTJ1-FhuA)	[5]
Human cell lines		
HEK293	Human embryonic kidney cells	ATCC CRL-1573

Spc^r, Gm^r, Tp^r, Km^r, *cam*, genes encoding resistance to spectinomycin, gentamicin, trimethoprim, kanamycin and chloramphenicol, respectively.

Table S4. Point mutations in MukB.

Name of mutant	Mutations
Hinge domain mutants	
P707	P707A
RH	R709 H710
PRH	P707A R709E H710A
GPSRH	G706A P707A A708A R709E H710A
D733	D733R
GSED	G668A S669A E670R D671A
PED	P731A E732A D733A
RR	R768E R771E
Head domain mutants	
RR	R186A R187A
DK	D193A K196A
EDE	E1386A D1387A E1388A
E1386	E1386A
E1387	E1387A
E1388	E1388A
RL	R1391A L1392A

Supplemental References

(1) Wang, Q., Mordukhova, E. A., Edwards, A. L., and Rybenkov, V. V. (2006) Chromosome condensation in the absence of the non-SMC subunits of MukBEF, *J Bacteriol 188*, 4431-4441 DOI 10.1128/JB.00313-06.

(2) Datsenko, K. A., and Wanner, B. L. (2000) One-step inactivation of chromosomal genes in Escherichia coli K-12 using PCR products, *Proc Natl Acad Sci U S A 97*, 6640-6645 DOI 10.1073/pnas.120163297.

(3) Dhamdhere, G., and Zgurskaya, H. I. (2010) Metabolic shutdown in Escherichia coli cells lacking the outer membrane channel TolC, *Mol Microbiol 77*, 743-754 DOI 10.1111/j.1365-2958.2010.07245.x.

(4) Petrushenko, Z. M., Zhao, H., Zgurskaya, H. I., and Rybenkov, V. V. (2016) Novobiocin susceptibility of MukBEF-deficient Escherichia coli is combinatorial with efflux and resides in DNA topoisomerases, *Antimicrob Agents Chemother 60*, 2949-2953 DOI 10.1128/AAC.03102-15.

(5) Krishnamoorthy, G., Leus, I. V., Weeks, J. W., Wolloscheck, D., Rybenkov, V. V., and Zgurskaya, H. I. (2017) Synergy between active efflux and outer membrane diffusion defines rules of antibiotic permeation into Gram-negative bacteria, *MBio 8*, e01172-01117 DOI 10.1128/mBio.01172-17.